International Journal of Mechanical and Electrical Engineering
ISSN: 3005-9615 (Print), ISSN: 3005-7132 (Online) | Volume 8, Number 2, Year 2026
DOI: https://doi.org/10.62051/ijmee.v8n2.04
Journal homepage: https://wepub.org/index.php/IJMEE/index

Applying Raked Wingtips in Sailplane Design

Haoyang Yu *

Department of Aeronautical and Aviation Engineering, The Hong Kong Polytechnic University, Hong Kong SAR, China

* Corresponding Author Email: 22101598d@connect.polyu.hk

ABSTRACT

Raked wingtips are widely used on passenger aircraft, but their potential application for low-speed aircraft such as sailplanes is less explored. Since wingtip treatments like winglets are commonly used on sailplanes, a raked wingtip can also be an alternative. In this study, the aerodynamic efficiency increase resulting from applying a raked wingtip to high-aspect-ratio sailplane wings, as well as the effectiveness of modern lifting line theory in optimizing the wingtip treatment design, were investigated. By conducting Reynolds-Averaged Navier-Stokes (RANS) Computational Fluid Dynamics (CFD) simulations on a GPU, the optimal raked wingtip configuration with a 25-degree leading-edge sweep angle was determined. The performance of the optimized raked wingtip is also compared with the baseline wing, baseline wing with a potential optimal winglet, and an extended wing. The results show that the optimal raked wingtip can improve the lift-to-drag ratio by nearly 2%, while the improvement of the selected winglet is only about 0.5%. Visualization of the flow field indicates that both the raked wingtip and the winglet can reduce the wingtip vortex. However, although the winglet can redirect the flow at the wingtip, the corner generates interference drag. Furthermore, the modern lifting line theory (implemented on the MachUpX program) was applied to optimize the raked wingtip and the winglet. For the raked wingtip, this theory can predict the general trend of the lift coefficient versus the sweep angle, but is unreliable in predicting the drag. For the winglet, the optimization effectiveness is limited due to its failure to simulate the complex 3D effect. The findings suggest that the raked wingtip is promising for sailplane applications, while also providing a general guideline for using modern lifting line theory to optimize raked wingtip and winglet design.

KEYWORDS

Wingtip Treatments; Sailplanes; Raked Wingtip; Winglet; Induced Drag; Computational Fluid Dynamics; Modern Lifting Line Theory.

1. INTRODUCTION

Wingtip treatments, such as winglets and raked wingtips, are widely used in commercial airliners intended to reduce the lift-induced drag and increase the fuel efficiency of the aircraft. Wingtip treatment reduces the induced drag by weakening the wingtip vortex. Since there is always a pressure difference between the bottom and the top of the wing, the flow would escape from the bottom to the top, thus causing the flow around the wing to gain a spanwise velocity which is opposite on the two sides of the wing. The opposite velocities meet at the trailing edge of the wing and roll up to two wing-tip vortices. These vortices will induce a downward velocity called downwash to the flow around the wing, which would reduce the effective angle of attack and twist the lift backward, contributing to the streamwise drag component. This drag is named induced drag, and if it can be reduced, a larger lift-to-drag ratio can be obtained, meaning that we can get less undesired drag when

generating the same amount of lift to balance the equal amount of weight. Therefore, the fuel consumption can be reduced.

The function of the winglet and the raked wingtip both reduces the influence of the wingtip vortices, but in a different manner. The winglet is the little wings that bend upwards at the two tips of the wing. They are usually designed to take aerodynamic loading and generate the sidewash to channel some of the spanwise velocity [1]. For raked wingtips, they are the part of the wing at the tip that has a higher sweep angle than the main wing and a gradually decreasing chord length. This kind of wingtip can increase the aspect ratio of the wing while not increasing too much wetted area. According to the lifting line theory, increasing the wing aspect ratio can also reduce downwash and induced drag. A raked wingtip can also redirect the wingtip vortices away from the main wing, weakening its influence [2].

As the sustainability of the aviation industry and the energy crisis have been given more and more attention, different wingtip treatments have become a hot research topic, especially in the field of transonic transport or passenger planes. The winglet was originally designed by Richard Whitcomb for commercial aircraft in the mid-1970s. Shortly after that, NASA installed winglets on the KC-135 Stratotanker aerial refueling tanker aircraft and conducted a thorough study to investigate the efficiency increase [3]. For some of the low-speed aircraft, winglets are also applied to increase the performance. For instance, sailplanes make use of the winglet to obtain a better cross-country soaring performance [1]. However, compared to winglets, raked wingtips are seldom used in low-speed aircraft, and there are only a few researchers who have studied the performance of raked wingtips in low Reynolds number conditions. Since the raked wingtip has a similar function to the winglet and may have advantages in some aspects, (such as being more efficient during the cruising stage [2], less interference drag caused by corners, and might having a larger lift coefficient respect to the original wing due to the increase in wing area), there might be some potential to apply this kind of wingtip to sailplanes not for competitions which do not have the restriction of their wing span. In addition, some studies imply that a winglet with a small cant angle, which is similar to the raked wingtip, may have good efficiency for slow-speed aircraft such as UAVs [4].

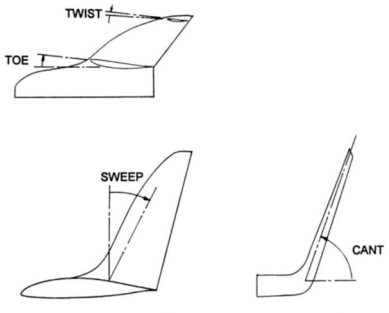

Figure 1. Definition of the toe, twist, sweep, and cant angles (Maughme,[1])

Researchers have developed various methods for optimizing the design of the winglet for low-speed aircraft. Since this design process required a large number of iterations, conducting CFD simulations could be computationally intensive. In addition, an experiment conducted for high aspect ratio sailplanes' wings can also bring about the problem of low Reynolds number. Therefore, inviscid potential flow methods are applied. For example, Maughme [5] and his team utilize the multiple lifting-line method, the full panel method, and relaxed-wake modeling. Naik and Ostowari [6] used a nonlinear panel method with wake relaxation to design the winglet. Kubryn [7] divided the winglet design process into 2D and 3D, by first obtaining the optimized winglet 2D layout using Munk theorem, and conducting the multi-point inverse design/optimization method to eliminate the 3D interference effect. All those methods are aimed at determining the key parameters of the winglet for

optimization, including the size, sweep angle, cant angle, toe angle, twist angle, and even the radius of the wing-winlet connection. The definition of the toe, twist, sweep, and cant angles is shown in Figure 1. It should be noted that different articles may have different ways to describe the toe angle (either measure relative to the zero-lift angle of attack of the airfoil or not). In this study, the toe angle is measured relative to the fuselage centerline, and the toe-out (leading edge outboard) is the negative toe angle, while the toe-in is the positive.

Despite so much research on the winglet for low-speed aircraft, such as the sailplane, there are fewer studies focusing on applying the raked wingtip to the sailplane and the inviscid low-computation cost methods to optimize it. Therefore, in this study, the probability of applying the raked wingtip to the sailplane to increase the aerodynamic efficiency is evaluated. This includes conducting a series of Reynolds-averaged Navier-Stokes (RANS) computational fluid dynamics (CFD) simulations to determine the optimized raked wingtip, evaluating the effectiveness of the modern lifting line theory for optimizing the raked wingtip and winglet, comparing the optimized wingtip with other wingtip treatment configurations, and detailed comparison and mechanism explanation between raked wingtips with different sweep angles.

2. METHODOLOGY

2.1. Geometries

To evaluate the efficiency of the winglet and the raked wingtip. CFD simulations are conducted between a high aspect ratio baseline wing without any wingtip treatment, a baseline wing with an optimized winglet attached, and a baseline wing with different raked wingtips having distinct sweep angles attached. The optimized sweep angle of the raked winglet can be found during the simulation and can be compared with the optimized winglet, which was determined by other studies. Since the design of the wingtip treatment is a trade-off process of reducing induced drag and the undesired result of the increase in profile drag, to get the same skin friction drag (a part of the profile drag), the winglet and different raked wingtips have the same area

For the high aspect ratio baseline wing, the aspect ratio is 25, and the wing span is 15m, intended to simulate the sailplane wing. The airfoil used was NACA 4412 for simplicity, and the quarter-chord sweep angle was set to zero. The taper ratio was set to 0.35, which was determined by a home-made program that calculates the induced drag efficiency factor for an arbitrary aspect ratio and taper ratio. This program used the Fourier series form of lifting line theory to calculate the factor.

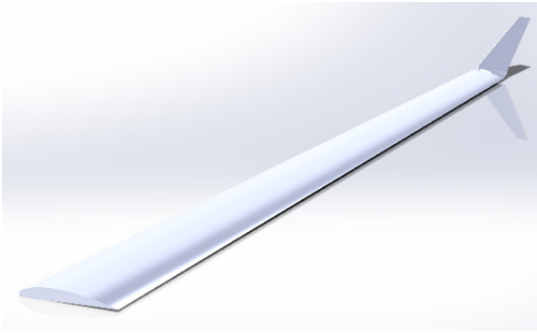

Figure 2. 3D model of the optimized winglet

In terms of the potential optimal winglet, although the famous researcher Mark D. Maughmer, who designed well well-performed winglet for sailplanes, published several papers about the design methodology for sailplane winglets, there were no specific data and parameters about the winglet, except the airfoil they used, which was the PSU 94-097 [1] [8]. Therefore, this airfoil was applied in the optimized winglet, and the planform shape employed a design from NASA. The optimized toe

angle and cant angle were determined by research studying this NASA winglet, which stated that the results are also valid for small Mach numbers such as 0.2 [9]. The angles are -4 and 75 degrees, respectively. Figure 2 and Figure 3 are the 3D models of the optimized winglet and the raked wingtip in a leading-edge sweep angle of 30 degrees.

The fluid domain is shown in Figure 4, which is constructed by a quarter sphere and a half cylinder. The radius and the height of the cylinder are 21m, about 35 times the mean chord, whose length is 0.6m.

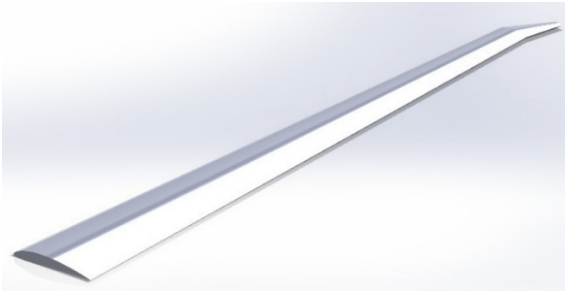

Figure 3. 3D model of the raked wingtip with a leading-edge sweep of 30°

2.2. CFD Turbulent Model and Methodologies

The turbulent model for conducting the 3D RANS CFD simulations is the Shear Stress Transport (SST) k-omega model. This model uses two equations relating to the k (Turbulence Kinetic Energy) and omega (Specific Dissipation Rate) to calculate the Reynolds stress and close the system.

CFD simulations, meshing, and post-processing, except for the GPU simulations for different sweep angles of the raked wingtip, are being conducted in the software Ansys Fluent 2024 R1 using a CPU. The GPU simulations for different sweep angles of the raked wingtip were conducted on a NVIDIA 2080Ti 22G GPU with the newest Ansys Fluent 2025 R2, whose updates focus on the implementation of GPU.

2.3. Mesh Independent Test

The meshes were generated by Fluent Meshing. As shown in Figure 5, the 3D mesh was generated using poly-hexcore with inflation layers for y plus constraints. The minimum cell length is about 4.22e-4m, and the maximum cell length is about 0.864m. A mesh convergent test was conducted using the model of the baseline wing to determine the suitable mesh cell number for acceptable accuracy and affordable computing cost. The convergent tests for lift coefficient and drag coefficient versus cell number are displayed in Figure 6. The suitable cell number selected for the baseline wing is about 5.081 million. For the mesh of the wing with the winglet and wingtip, though having sight different cell number, the size controls in the mesh generating process are identical, ensuring the same degree of accuracy.

2.4. CFD Settings

The CFD simulation was conducted with a free stream velocity of 60 m/s. The air density and the dynamic viscosity were set to 1.225 kg/m3 and 1.7894e-5 kg/(ms). Due to the limited computing power of the CPU (Intel i7 on a laptop), the iterations for each CPU simulation were set to 500, resulting in residuals around 2e-5, while for the GPU, the iteration number was set to 1000, with the residuals 2e-5 to 7e-6. That is because the Fluent run on GPU is about 40 times faster than that of CPU. (It took about 7 hours for 500 iterations for CPU and approximately 20 minutes for GPU.) The GPU simulation conducted a full range evaluation of the raked wingtip with leading edge sweep angle between about 0 and 60 degrees (quarter-chord sweep angle between about -5 and about 58 degrees), with a 10-degree step, while the CPU simulations were done only for the 3 sweep angles close to the

optimal sweep angle. The mesh-independent test, simulations for the baseline wing, as well as simulations for the potential optimal winglet, were conducted on the CPU.

2.5. Modern Lifting Line Theory

The lifting line theory was proposed by Prandtl in 1918. It is a convenient tool to estimate the efficiency of the finite wing. However, this theory also has some limitations. After a year of research, the lifting line theory can be applied to a broader scenario. In 2000, Phillips and Snyder [10] developed the modern adaptation of the lifting line theory, which is the P-S method. Recently, the theory was improved by Reid and Hunsaker (2021) (R-H method) and further finalized by Goates and Hunsaker (2023) (G-H method), who also developed a program called MachUpX based on the modern lifting line theory. This theory distributes the joint horseshoe vortices along the wing, with the bound vortices aligned with the quarter-chord line. Therefore, the grid is one-dimensional, and the computational cost is relatively low. This theory is able to predict the efficiency of the wing with arbitrary sweep, dihedral, and twist. The effectiveness of the program MachUpX to optimize the raked wingtip and winglet design was evaluated.

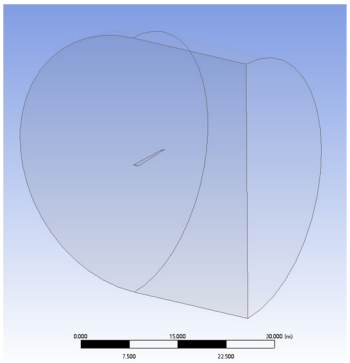

Figure 4. The flow domain for CFD simulation

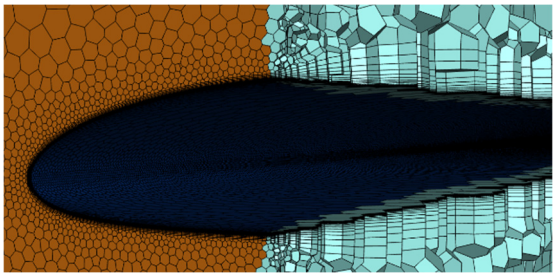

Figure 5. The 3D mesh for CFD simulation

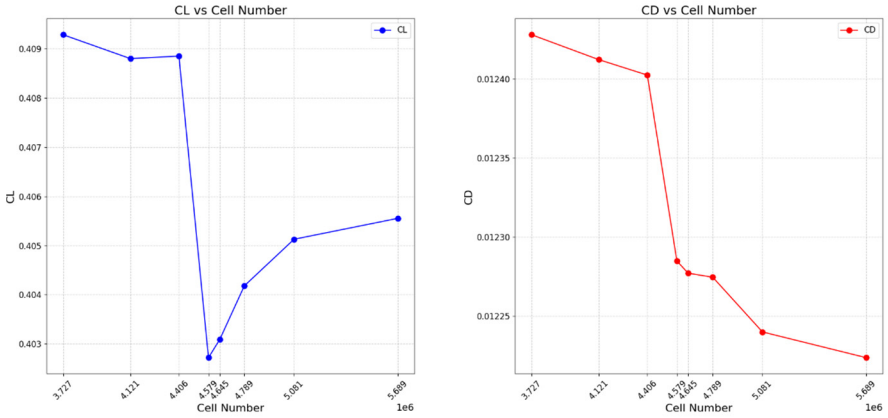

Figure 6. CL and CD versus the mesh cell number

3. RESULTS AND DISCUSSION

3.1. The Optimized Wingtip

It should be noted that the coefficients in this study are all calculated based on the area of the baseline wing. Figure 7 shows the GPU calculated lift coefficient (CL), drag coefficient (CD), and the lift-to-drag ratio (L/D) when varying the quarter-chord sweep angle of the raked wingtip. It is obvious that the 25.05-degree quarter-chord sweep angle (or 30-degree leading edge sweep angle) raked wingtip is the optimal one. It can also be seen that the CL, CD, and the L/D have the same trend when increasing the sweep angle.

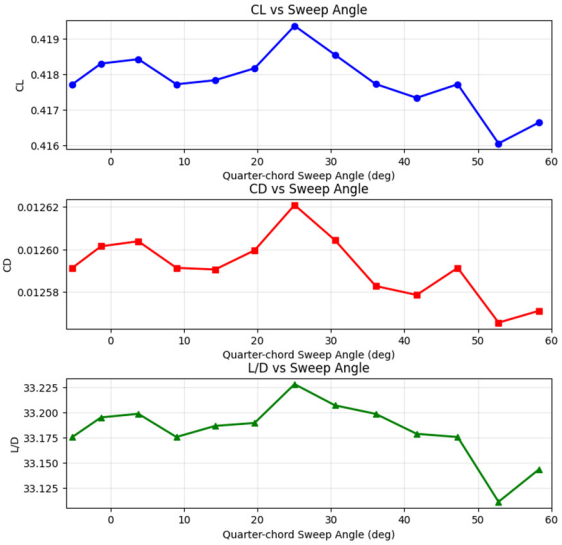

Figure 7. The GPU results of CL, CD, and L/D versus the quarter-chord sweep angle for the raked wingtip

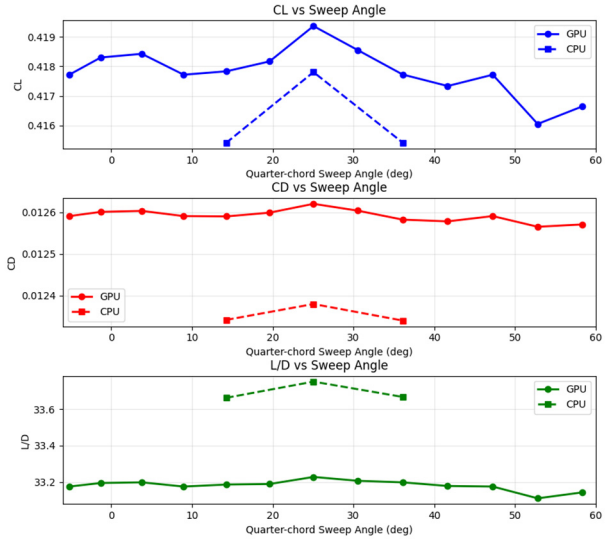

Figure 8. The comparison of the GPU and CPU results of CL, CD, and L/D versus the quarter-chord sweep angle

Figure 8 presents a comparison between the full-range GPU simulation and the 3-point CPU simulation, which is close to the optimal sweep angle. According to the figure, they have a similar

trend but different values. Although the reference value, constants in the turbulent model, and the boundary condition are all set to the same value, there are still some differences between the GPU and CPU results. However, since the difference is not significant and the trend is the same, the GPU results can be regarded as agreeing with those of the CPU.

3.2. Modern Lifting Line Theory for Predicting Optimal Raked Wingtip

Figure 9 shows the lift coefficient, drag coefficient, and the lift-to-drag ratio calculated from the modern lifting line for different quarter-chord sweep angles. However, since the profile drag is determined in the MachUpX by airfoil profile drag estimated using the boundary layer theory in Xfoil, the drag coefficient may not be accurate. Combining the results from Figures 7 and 9, it can be concluded that the drag calculation in MachUpX is unreliable for both the data and the trends, but the trend for the lift calculation generally matches the GPU CFD results. Both data gradually increase before the maximum CL point and drop significantly after the optimal point. Most importantly, the optimal point is close, with the CFD data at 25 degrees and the MachUpX data at 15 degrees. However, the decrease of around 10 degrees and the fluctuation after 40 degrees could not be predicted by the theory. Additionally, there are deviations in the CL data, since the values are usually overestimated.

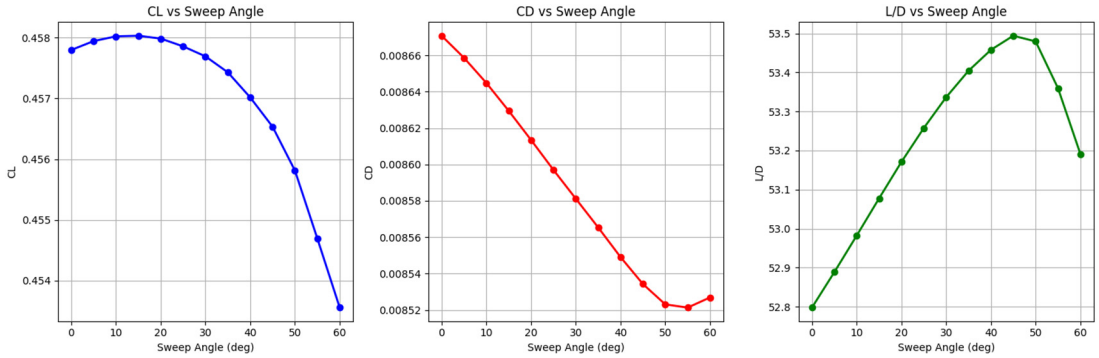

Figure 9. The modern lifting line theory results of CL, CD, and L/D versus the quarter-chord sweep angle

3.3. The Winglet

According to Kubrynski [7], it is beneficial to have the ios-bar line run along the span of the winglet, as shown in Figure 10 (b). If a region with negative pressure is followed by a region with a high pressure gradient, as shown in Figure 10 (a), the efficiency will decrease due to the aerodynamic interference, and there is also a risk of flow separation. The current winglet configuration in Figure 11 (a) indeed has a negative pressure region, indicating that this potential optimal winglet may not be the best configuration. However, the negative pressure is not significant, so the velocity profile in the boundary layer shows no sign of flow separation, as shown in Figure 11 (b).

3.4. Modern Lifting Line Theory for Predicting Optimal Winglet

The modern lifting line theory was applied to find the optimized winglet by testing various sweep, cant, and toe angles. To ensure a smooth transform between the winglet and raked wingtip, the NACA4412 airfoil is applied to all the wing segments. However, the modern lifting line theory was limited in optimizing the winglet. That is, first, due to the pre-proofed unreliability of the drag prediction. Since the major effect of the winglet is to reduce the total drag, this strictly limits the effectiveness of the modern lifting line theory. Second, it can be observed from Figure 12 that the CL always increases when reducing the sweep or cant angle, or increasing the toe angle. These are all aligned with 2D effects, as follows: first, lift will increase when the airfoil slightly increases the angle of attack; second, CL will decrease when the wing platform has a large sweep angle; third, CL will

increase when the wing has a larger projection area. That might indicate that the modern lifting line theory fails to take the complex 3D effect into consideration, which is actually the nature of the classical lifting line theory.

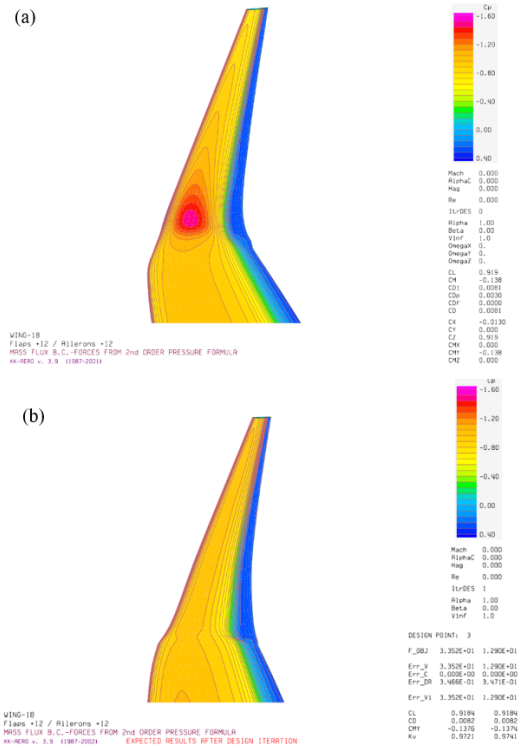

Figure 10. The comparison of the poorly designed winglet with a negative pressure region (a), and the well-designed winglet with constant pressure along the span (b)

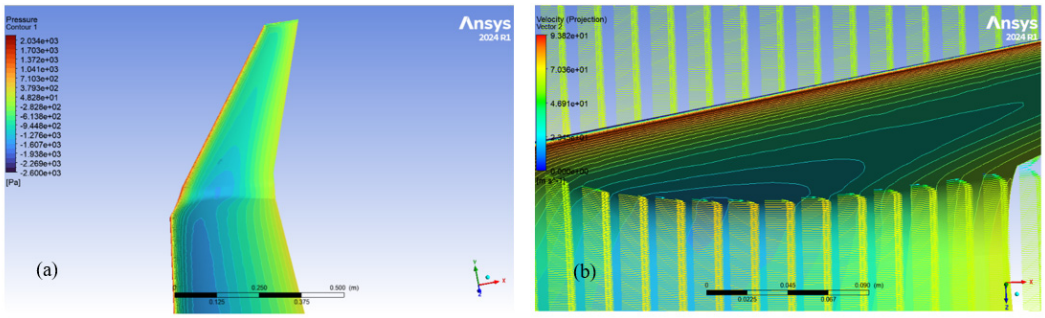

Figure 11. The pressure contour of the selected winglet (a) and the velocity vector around the winglet surface (b)

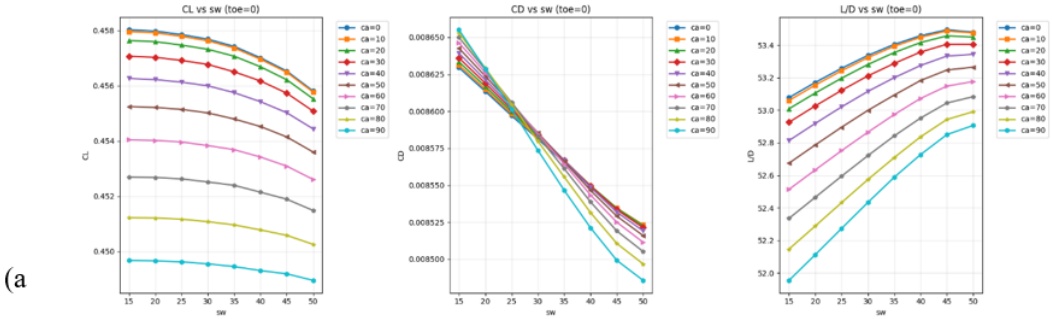

Figure 12. (a) CL, CD, and L/D versus various sweep angles (all quarter-chord) for different cant angles at toe angle = 0

(b)

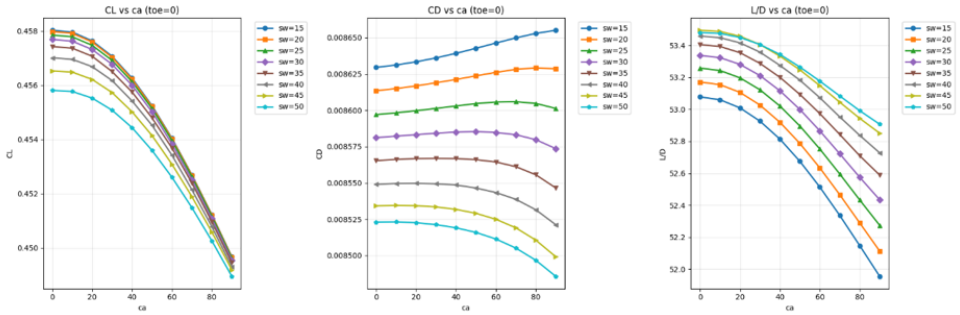

Figure 12. (b) CL, CD, and L/D versus various cant angle for different sweep angles at toe angle = 0

(c)

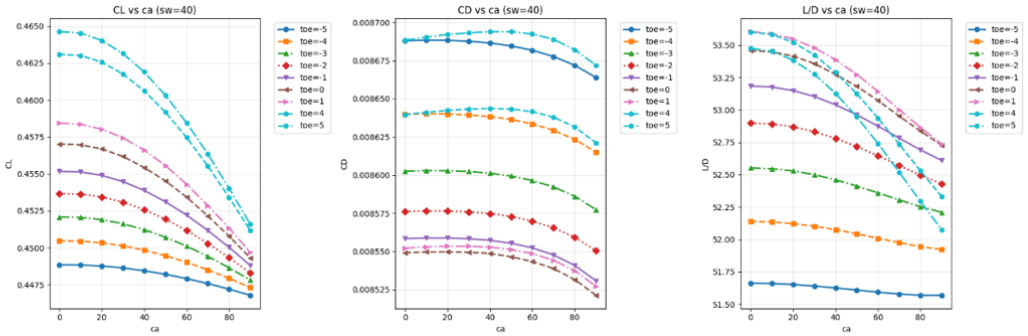

Figure 12. (c) CL, CD, and L/D versus various cant angles for different toe angles at sweep angle = 40

3.5. The Comparison between Wingtip Treatments

The CFD results for the baseline wing, baseline wing with optimal winglet, baseline wing with optimal raked wingtip, and extended wing are shown in Table 1. It can be observed that the efficiency improvement for the raked wingtip is higher than winglet. However, the percentage of improvement for the raked wingtip is still quite low, less than 2%. Additionally, the improvement of the optimal winglet can be ignored.

The extended wing was constructed by directly extending the leading and trailing edges of the wing to the same span as the wingtip, making its wet area larger than the wingtip. (since the wingtip has a smaller tapered ratio). The extended wing had a negative influence on the lift-to-drag ratio of -2.3%. Although the CL of the extended wing is the highest, the CD is also the highest, leading to a lower lift-to-drag ratio. Therefore, both wingtip treatments are more beneficial than simply extending the wing to increase the aspect ratio.

The mechanics of efficiency improvement can be explained by the velocity contours and iso-surface of the Q value. Figure 13 shows the velocity w contour for the baseline wing, the baseline wing with the wingtip, and the baseline wing with the winglet, and Figure 14 shows the velocity v contour for the same sequence. All the figures are plotted in the same velocity legend range as displayed at the left of all the figures. These figures indicate that the downwash slightly reduces after adding the raked wingtip, while the downwash decreases remarkably for the winglet with the center of the vortex moved up to the tip of the winglet. Although the effect of the downwash is less significant for the winglet, the drag coefficient remains higher than for the other two configurations. That might be because the corner of the winglet generates additional interference drag, despite having a smooth transition curve. Moreover, since the raked wingtip can generate additional lift, the lift-to-drag ratio for the wing with a raked wingtip is higher. Figure 15 a-c shows the iso-surface for Q = 1e5, indicating that the regions possess a high Q value, thus having a strong vortex. It can be seen from the figures that the wing with a raked wingtip and winglet has smaller iso-surfaces of Q = 1e5 compared to the

baseline wing, which implies that it has weaker wingtip vortices than the baseline wing. It can also be observed that the winglet also disperses the Q or the vortex around the winglet.

Table 1. CFD results for the baseline wing, baseline wing with optimal winglet, and baseline wing with optimal raked wingtip

	baseline	Wingtip (optimal)	winglet	Extended wing
CL	4.051E-01	4.178E-01	4.157E-01	4.208E-1
CD	1.224E-02	1.238E-02	1.250E-02	1.276E-2
L/D	3.310E+01	3.375E+01	3.325E+01	3.297E+1
% Improve		1.97%	0.46%	-2.30%

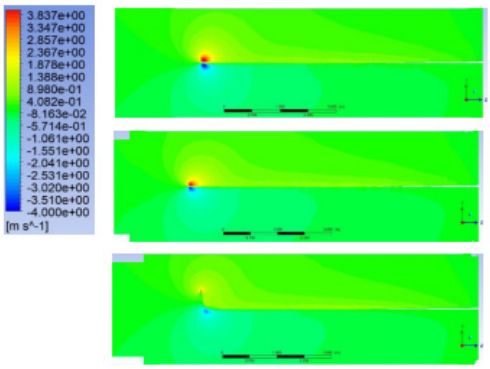

Figure 13. Velocity w contour for baseline wing, wing with wingtip, and wing with winglet

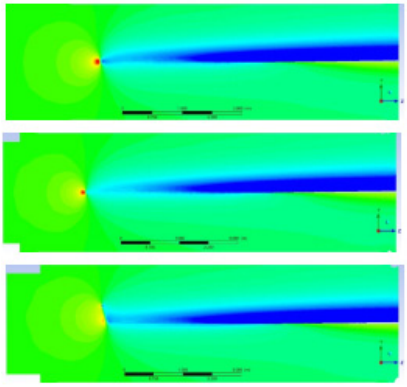

Figure 14. Velocity v contour for baseline wing, wing with wingtip, and wing with winglet

Figure 16 shows the x-direction vorticity contour of the raked wingtips in different quarter-chord sweep angles. The contours were plotted at different distances from the wing root leading edge, which is 0.4m, 0.7m,1m, and 1.3m, respectively. It can be seen that large vorticity is usually generated immediately after the wingtip, and the vorticity would dissipate gradually, achieving a low vorticity level after about 0.7m behind the wingtip.

Figure 16 can also prove the lift-to-drag ratio shown in Figure 7. For the low-sweep angle raked wingtip, the wingtip vortex is generated close to the main wing; thus, the downwash significantly influences the main wing, resulting in relatively low efficiency. However, the wing with a small sweep is beneficial for generating lift, ensuring that efficiency remains adequate. For a mid-sweep angle raked wingtip (like 25.05 degrees), the wingtip vortex is still concentrated at the wingtip, which is relatively away from the main wing, thus having less influence and achieving a high efficiency.

However, for the high sweep angle raked wingtip, instead of concentrating most of the vorticity at the wingtip, remarkable amounts of vorticity are generated along the trailing edge of the highly swept part (as shown in the 0.7m position contour in Figure 16 (d)), affecting the main wing. In addition, the sweep angle can influence the lift generated by the wing; the lift coefficient is usually assumed to reduce by multiplying the cos value of the quarter chord sweep angle. This is also indicated in Figure 17 (d), where the wingtip section has a larger pressure on the section side.

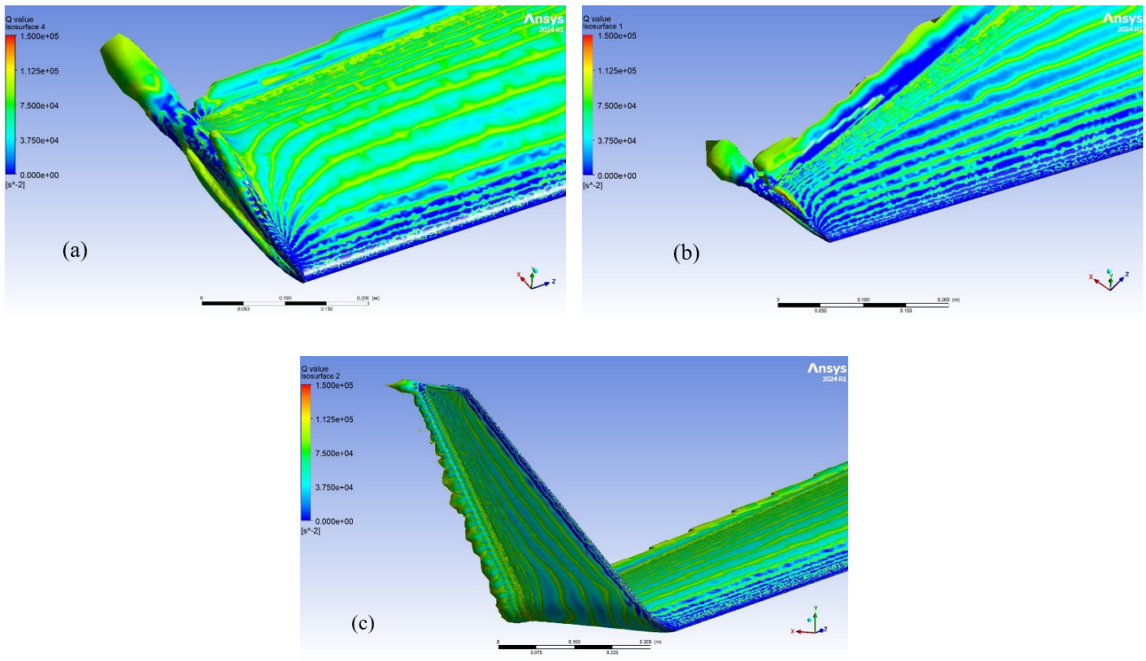

The comparison between raked wingtips with different sweep angles

Figure 15. (a-c). Q=1e5 iso-surface for baseline wing (a), wing with raked wingtip (b), and wing with winglet (c)

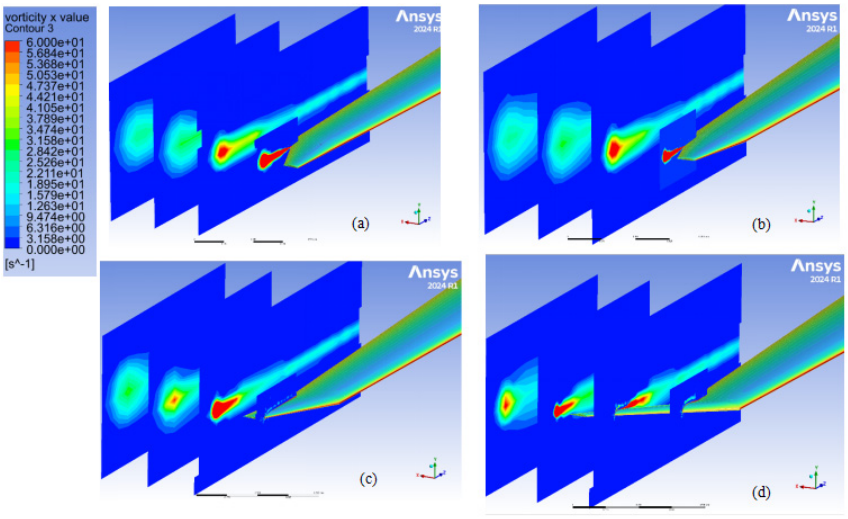

Figure 16. (a-d). x-direction vorticity contours of raked wingtip with quarter-chord sweep angle - 5.19 degrees (a), 3.79 degrees (b), 25.05 degrees (c), 52.81 degrees (d)

It can also be inferred from Figure 17 that the 25.05 degrees and 3.79 degrees raked wingtips are likely to have an elliptical lift distribution on both the main wing and the raked wingtip part, which might be the reason why their lift-to-drag ratio are the highest two.

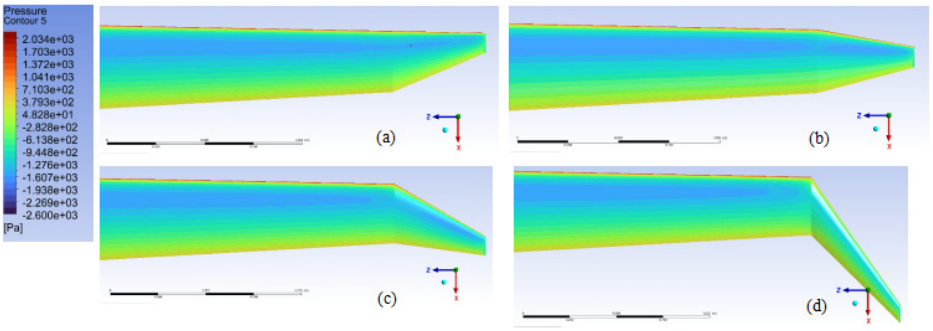

Figure 17. (a-d). pressure contour of raked wingtip with quarter-chord sweep angle -5.19 degrees (a), 3.79 degrees (b), 25.05 degrees (c), 52.81 degrees (d)

4. CONCLUSION AND FUTURE WORK

This study comprehensively evaluated the potential of raked wingtips for high-aspect-ratio sailplane wings and assessed the effectiveness of the modern lifting line theory in optimizing such wingtip treatments. Through a series of RANS CFD simulations and modern lifting line calculations implemented on MachUpX, the following conclusions can be drawn:

Performance of Raked Wingtip: The raked wingtip demonstrates promising potential for sailplane application. An optimal configuration with a 25-degree quarter-chord sweep angle was identified, which improved the lift-to-drag ratio by nearly 2% compared to the baseline wing, outperforming the selected "potential optimal" winglet, which only yielded a 0.5% efficiency gain. The CFD results indicate that the selected winglet might not be the optimal one, and the flow field analysis revealed that while the winglet successfully elevates and weakens the tip vortex, the junction between the wing and the winglet generates significant interference drag, offsetting its induced drag benefits. Furthermore, simply extending the wing span to match the raked wingtip's projection was found to be detrimental to performance due to a disproportionate increase in drag.

Capabilities and Limitations of Modern Lifting Line Theory: The modern lifting line theory, as implemented in MachUpX, showed mixed results in the optimization process.

For the raked wingtip, the theory was able to predict the general trend of the lift coefficient variation with sweep angle and provided a rough estimate of the optimal sweep region, despite an overall over-prediction of lift. However, its drag prediction was unreliable, both in magnitude and trend, severely limiting its utility for direct optimization where drag reduction is a crucial goal.

For the winglet, the theory's limitations were more pronounced. The predicted trends for lift with varying sweep, cant, and toe angles aligned primarily with 2D aerodynamic principles and failed to capture the critical 3D interference effects at the wing-winglet junction. This failure to model complex 3D flows renders it inadequate for reliable winglet optimization.

For the comparison of different raked wingtips with distinct sweep angles, the efficiency improvement by the raked wingtip is attributed to their ability to effectively weaken and redirect the wingtip vortex away from the main wing. Since the raked wingtips that have a too low or too high sweep angle would generate vortices close to the main wing, their efficiency is lower than the mid-sweep raked wingtip.

There are four aspects for future investigations. In this study, a potential optimal winglet was chosen based on the winglet optimization research of the KC-135 Stratotanker (a swept-wing aircraft) under a similar Mach number. This winglet configuration may not be the optimal one when applying it to the high-aspect ratio sailplane wing. Indicating that the different wings should have their own optimal winglet design. The future study may first involve applying GPU-powered RANS CFD to test

different winglet configurations and find the optimal one. In this way, the effectiveness of the CL prediction of the modern lifting line theory can also be evaluated.

Second, since the performances of the different wingtip treatments were only tested at zero angle of attack, they need to be tested at various angles of attack according to the mission profile of the sailplanes, to ensure the optimal treatment works for most angles of attack.

Third, 3D Large Eddy Simulation (LES) or the Detached Eddy Simulation (DES) can be applied to increase the accuracy of the simulation results, since the current RANS may reach a limit with a residual of 1e-5, which cannot decrease further.

Last but not least, we may consider applying the experimental data or high-fidelity simulation results to replace the airfoil data currently calculated by the Xfoil, thus more accurately calculating the viscous effect. Since the modern lifting line theory cannot capture the complex 3D effect, it might be considered to further modify the theory, enabling it to not only predict the downwash, but also the wingtip vortex and the aerodynamic interference.

In summary, the raked wingtip presents itself as a potentially more efficient alternative to the winglet for the specific high-aspect-ratio sailplane wing investigated. Meanwhile, the modern lifting line theory serves as a useful preliminary tool for analyzing lift trends in raked wingtips, but it is not sufficient for final design optimization due to its inaccurate drag prediction and inability to model key 3D interference effects. Future work should focus on integrating high-fidelity CFD airfoil results into modern lifting line theory, optimizing both raked wingtips and winglets across a range of angles of attack, and on developing more sophisticated low-order models that can account for strong 3D interference phenomena.

REFERENCES

[1] M. D. Maughme, "The Design of Winglets for Low-Speed Aircraft," in Sport Aviation Symposium, Milano, Italy, 2005.

[2] Y. Gharbia, J. F. Derakhshandeh, M. M. Alam, and A. M. Amer, "Developments in Wingtip Vorticity Mitigation Techniques: A Comprehensive Review," Aerospace, vol. 11, no. 1, 2023, doi: 10. 3390/aerospace11010036.

[3] R. R. Meyer, Jr. and P. F. Covell, "Effects of Winglets on a First-Generation Jet Transport Wing. VII—Sideslip Effects on Winglet Loads and Selected Wing Loads at Subsonic Speeds for a Full-Span Model," NASA, Washington, D.C., NASA Technical Paper 2619, Sept. 1986.

[4] E. Nikolaou, S. Kilimtzidis, and V. Kostopoulos, "Winglet Design for Aerodynamic and Performance Optimization of UAVs via Surrogate Modeling," Aerospace, vol. 12, no. 1, 2025, doi: 10.3390/aerospace12010036.

[5] M. D. Maughmer, "Design of Winglets for High-Performance Sailplanes," Journal of Aircraft, Nov. 2003.

[6] D. A. Naik and C. Ostowari, "Effects of Nonplanar Outboard Wing Forms on a Wing,"Journal of Aircraft, vol. 27, no. 2, pp. 117-122, Feb. 1990.

[7] K. Kubrynski, "Wing-Winglet Design Methodology for Low Speed Applications," in 41st Aerospace Sciences Meeting and Exhibit, Reno, NV, USA, Jan. 6-9, 2003, doi: 10.2514/6.2003-215.

[8] M. D. Maughmer, T. S. Swan, and S. M. Willits, "The Design and Testing of a Winglet Airfoil for Low-speed Aircraft," Journal of Aircraft, vol. 39, no. 4, 2002.

[9] J. Halpert, D. Prescott, T. Yechout, and M. Arndt, "Aerodynamic Optimization and Evaluation of KC-135R Winglets, Raked Wingtips, and a Wingspan Extension," in 48th AIAA Aerospace Sciences Meeting Including the New Horizons Forum and Aerospace Exposition, 2010.

[10] W. F. Phillips and D. O. Snyder, "Modern Adaptation of Prandtl's Classic Lifting-Line Theory," Journal of Aircraft, vol. 37, no. 4, pp. 662-670, July–August 2000.

[11] J. T. Reid and D. F. Hunsaker, “A General Approach to Lifting-Line Theory, Applied to Wings with Sweep,” Utah State University, Logan, UT, USA, Tech. Rep., 2021.

[12] C. D. Goates and D. F. Hunsaker, "Modern Implementation and Evaluation of Lifting-Line Theory for Complex Geometries," Journal of Aircraft, vol. 60, no. 2, pp. 490-508, 2023.